

One Trajectory, One Token: Grounded Video Tokenization via Panoptic Sub-object Trajectory

Chenhao Zheng^{1,2}, Jieyu Zhang^{1,2}, Mohammadreza Salehi^{1,2}, Ziqi Gao¹,
Vishnu Iyengar¹, Norimasa Kobori³, Quan Kong³, Ranjay Krishna^{1,2}

¹University of Washington, ²Allen Institute for Artificial Intelligence, ³Woven by Toyota, Inc

Abstract

Effective video tokenization is critical for scaling transformer models for long videos. Current approaches tokenize videos using space-time patches, leading to excessive tokens and computational inefficiencies. The best token reduction strategies degrade performance and barely reduce the number of tokens when the camera moves. We introduce grounded video tokenization, a paradigm that organizes tokens based on panoptic sub-object trajectories rather than fixed patches. Our method aligns with fundamental perceptual principles, ensuring that tokenization reflects scene complexity rather than video duration. We propose TrajViT, a video encoder that extracts object trajectories and converts them into semantically meaningful tokens, significantly reducing redundancy while maintaining temporal coherence. Trained with contrastive learning, TrajViT significantly outperforms space-time ViT (ViT3D) across multiple video understanding benchmarks, e.g., TrajViT outperforms ViT3D by a large margin of 6% top-5 recall in average at video-text retrieval task with 10x token deduction. We also show TrajViT as a stronger model than ViT3D for being the video encoder for modern VideoLLM, obtaining an average of 5.2% performance improvement across 6 VideoQA benchmarks while having 4x faster training time and 18x less inference FLOPs. TrajViT is the first efficient encoder to consistently outperform ViT3D across diverse video analysis tasks, making it a robust and scalable solution.

1. Introduction

With video comprising over 80% of global internet traffic [56], designing efficient video encoders is essential. Since the transformer architecture [58] is now the standard for encoding video data [35, 43], efficient design hinges on the tokenization algorithm. Today’s de-facto tokenization algorithm splits the video tensor into space-time patches [43] as shown in Fig.1(a). In other words, the longer

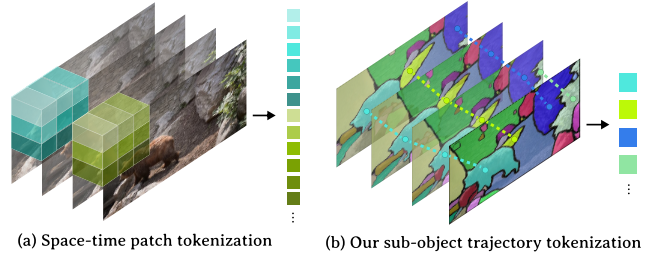


Figure 1. (a) Traditional video tokenization divides a video into space-time patches, leading to large number of redundant tokens. (b) We propose to represent a video via panoptic sub-object trajectory, where each token represents a trajectory.

the video, the more tokens are extracted.

This tokenization paradigm introduces significant challenges: First, it leads to memory bottlenecks, as a one-minute video sampled at just one frame per second could produce over 6000 tokens [2]. Second, it does not respect the scene complexity, treating all videos equally regardless of their visual content. For instance, a one-minute video of a static office desk without any motion produces the same number of tokens as a one-minute video of a football match with high-speed athleticism. Third, it places a heavy burden on the transformer encoder to connect disjoint tokens across frames as a singular concept (e.g., the same office desk). Researchers have proposed various token merging strategies to mitigate these challenges, but they are either not content-aware [2, 3, 48] or perform poorly when the camera taking the video is moving [11].

We depart from patch-based tokenization to propose a new paradigm of *grounded video tokenization*. Instead of naively splitting videos into patches to be tokenized, we align tokenization with the fundamental perceptual principles governing object perception and motion [45, 54, 59] by organizing tokens to correspond to panoptic sub-object trajectories. Rooted in Spelke’s core cognitive principles [54] and the Gestalt Principle of *common fate*, we treat object parts as coherent entities that persist over time (Fig. 1b). By

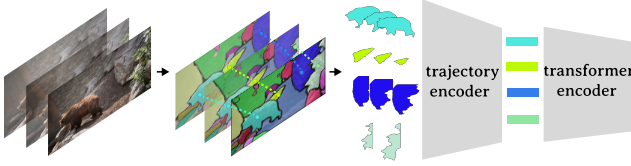


Figure 2. **Overview of TrajViT.** Given a video, we first panoptically extract the trajectories for all objects. Our trajectory encoder converts these dynamic object trajectories into fixed sized embeddings, which serve as the input to the transformer encoder.

correlating token count with the number of distinct panoptic sub-object trajectories—rather than frame count—our method directly reflects the complexity of a scene in terms of its constituent objects and their interactions, allowing efficient processing of long sequences. Moreover, because our tokenization divides a video into objects rather than raw pixel divisions, it remains robust to variations in lighting conditions, occlusions, and camera movements—a challenge for patch-based tokenizers [4, 26, 27].

We operationalize this paradigm by designing *TrajViT*, a video encoder with grounded video tokenization and a standard transformer encoder (Fig. 2). Given a video, TrajViT extracts panoptic trajectories for all object parts and converts each into a fixed-size token. All tokens are then processed by a transformer encoder. In addition to its content-aware nature, TrajViT offers several advantages: (1) it significantly reduces the number of tokens—by an average of $10\times$ in the Panda dataset [8]—compared to space-time patch tokenization. (2) the tokens are organized into semantically meaningful units with no temporal redundancy, both of which facilitate high-level reasoning about object interactions for the encoder; (3) it makes the tokenization invariant to low-level visual variations in lighting and camera motion, leading to improved performance in video understanding tasks despite using fewer tokens.

In designing TrajViT, our core technical challenge lies in developing an efficient trajectory generation pipeline that can extract trajectories panoptically with sub-object granularity, and a module that can encode distinct trajectories into fixed-size tokens. We first develop a trajectory generation pipeline that integrates off-the-shelf segmenter [6] and tracker [47] through a parallelizable algorithm, which generates panoptic sub-object trajectories while minimizing latency caused by the tracking model. We also design a lightweight *trajectory encoder* that maps each distinct trajectories with variable number of pixels and appearing frames into fixed-size tokens, while maintaining the information about their appearance and temporal position variations. TrajViT can also process image data by treating each image segment as a trajectory of length one, allowing seamless joint training with both videos and images. Finally, we train TrajViT with a contrastive learning objective

on a large-scale video/image-text dataset.

We compare TrajViT with standard ViT with space-time patch tokens (ViT3D) and state-of-the-art token merging methods on a wide range of video understanding tasks, including video-text retrieval, spatial-temporal detection, action classification, and temporal clip retrieval. It outperforms ViT3D in all tasks, while all token merging baselines underperform ViT3D on average. At the largest training scale, TrajViT surpasses ViT3D by a significant margin of 6% in top-5 recall with $10\times$ fewer tokens. TrajViT is particularly effective because most video tasks are object-centric or require fine-grained recognition. For efficiency, despite the additional overhead of trajectory generation, TrajViT trains faster, consumes less GPU memory, and performs faster inference for videos with more than 64 frames.

Lastly, we train two VideoLLMs by connecting Llama3 with TrajViT and ViT3D as video encoders. On six VideoQA benchmarks, the average accuracy of the TrajViT-LLM surpasses ViT3D-LLM by 5.24%, while being trained 4x faster and running at $18\times$ fewer inference FLOPs. On the MovieChat benchmark [52] for long video evaluation, TrajViT-LLM displays better accuracy and efficiency than ViT3D-LLM when we scale up the number of input frames.

2. Related Work

Video tokenization. In the field of video understanding, ViViT [2] introduced spatio-temporal patches to tokenize and process videos with transformers more efficiently than tokenizing video frames independently [39, 46]. Subsequent research has exploited the temporal redundancy of videos and improved tokenization efficiency through patch dropping [11, 15, 69] or alternative input forms such as motion vector tokenization [23]. Recent researches like [11] has made tokenization more content-aware with token counts adapting to video complexity, but performs poorly when the camera taking the video is moving.

Efficient video encoders. Prior work has improved video encoder efficiency through approaches like token merging or pruning in intermediate transformer layers [3, 5, 10, 34, 44], compressing content into fewer learnable tokens [33, 42, 48, 70] or via sampling tokens based on importance scores [14, 60]. Unfortunately, the reduction in tokens is often accompanied by a reduction in model performance [2, 3, 11]. Other works have introduced architectural changes, such as modifying the attention mechanism [32, 50] or implementing state-space models to improve video modeling efficiency [31]. Our work focuses on token reduction without modifying transformer architecture.

Efficient video large language models. In the context of large video language models (VideoLLMs), to reduce the number of video tokens in the language model’s context length, previous research has proposed merging or dropping vision encoder output tokens [7, 66]. This is commonly

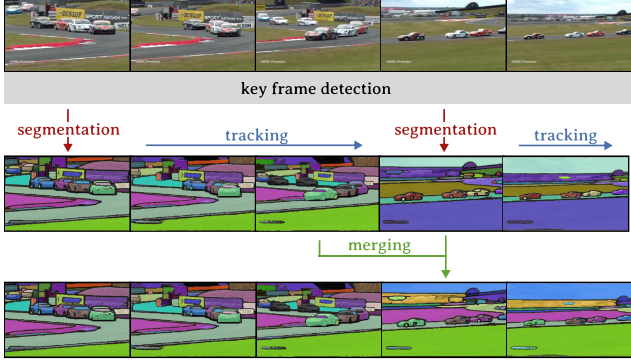


Figure 3. **Our parallel trajectory generation pipeline.** We use key frame detection to break a video into subclips. We segment and track objects in each clip in parallel and finally merge objects between clips. This paradigm captures objects that emerge over time while reducing overall tracking latency.

accomplished via learnable components such as perceiver resampler [1, 22] or through instruction conditioned token pruning [29, 30, 33, 49]. Notably, our approach is orthogonal to all these methods as we modify the tokenization before the transformer models.

3. Grounded Video Tokenization

Our approach aims to represent videos using semantically meaningful and compact tokens derived from panoptic sub-object trajectories. As illustrated in Fig. 2, we panoptically extract trajectories for all objects in a video and convert them into fixed-size embeddings to be used as the transformer encoder input. We find that trajectory extraction and encoding each pose distinct challenges. First, existing tracking solutions, which propagate segmentation masks from frame to frame, cannot handle newly appearing objects mid-video and are prone to long propagation time [9, 47, 65], necessitating a new trajectory generation pipeline. Second, the trajectories we generated can contain a varying number of pixels and appear in a varying number of frames, but the final representations need to be fixed-size embeddings to be compatible with the transformer architecture, requiring a new trajectory encoding module. We detail how we tackle these challenges in this section.

3.1. Panoptic Sub-object Trajectory Extraction

Our objective is to accurately segment and track all objects in a video—including backgrounds—while keeping the process efficient. We design a pipeline that couples an off-the-shelf segmentation and tracking model, can capture objects that emerge over time, and can be parallelized to reduce latency.

Discovering objects by segmenting key frames. Given a video of length T with time index $t \in \{1, \dots, T\}$,

we begin by selecting key frames $\{\hat{t}_i\}_{i=1}^K$ where new objects are likely to appear. Specifically, we compare the color histogram and luminance intensity between consecutive frames and flag those exceeding a manual threshold (details in supplementary). Then, we panoptically segment each key frame to capture all objects. We employ the DirectSAM model [6] as it is lightweight with 84M parameters and can produce fine-grained segments in one forward pass with consistent granularity across images, reducing the risk of merging failure in the later merging stage. We denote the segmentation mask derived in key frames as $\{M_{\hat{t}_i}\}_{i=1}^K$.

Tracking objects within each clip. The detected key frames naturally partition the video into multiple clips. Within each clip $\hat{t}_i \leq t < \hat{t}_{i+1}$, we employ an off-the-shelf tracker (SAM2 [47]) to propagate the segmentation mask $M_{\hat{t}_i}$ from the key frame \hat{t}_i to subsequent ones. This per-clip process can be executed in parallel for a batch of clips for efficiency (Fig. 3). In practice, we additionally split a clip at the midpoint if its length exceeds a certain threshold to shorten the propagation time. We use hiera-small variants of SAM2 with 46M parameters.

Merging objects between consecutive clips. Finally, we link the identities of objects between consecutive clips. Specifically, we perform an additional tracking step from the final frame of a clip ($\hat{t}_{i+1} - 1$) to the first frame of the subsequent clip (\hat{t}_{i+1}), generating a propagated mask $M'_{\hat{t}_{i+1}}$. We then compare each segment in $M'_{\hat{t}_{i+1}}$ with those in the original key frame mask $M_{\hat{t}_{i+1}}$. If the Intersection over Union (IoU) for any pair of segments exceeds a threshold of 0.8, we consider them to represent the same object and merge their trajectories.

This split-track-merge pipeline efficiently discovers and tracks objects across entire videos. The visualizations of generated trajectories are shown in supplementary. While we observe occasional inconsistent tracking, i.e., segments of the same object in consecutive clips being tagged as different trajectories due to imperfect merging, it seldomly hurts model performance because we find that these inconsistencies often coincide with situations where the object undergoes a large appearance change. In such cases, creating a new trajectory might benefit downstream tasks, as it accounts for significant changes in objects.

3.2. Video Encoding with Trajectory Tokens

We aim to obtain fixed-size representations of trajectories and utilize them as input for a transformer model. To achieve this, we develop a *trajectory encoder* that produces an appearance embedding and a temporal position embedding for each trajectory (Fig. 4).

Trajectory appearance encoding. For trajectory appearance encoding, we first extract hierarchical visual features from each frame. Given a video consisting of frames $\{I_t\}_{t=1}^T$, we apply a lightweight convolutional network [20]

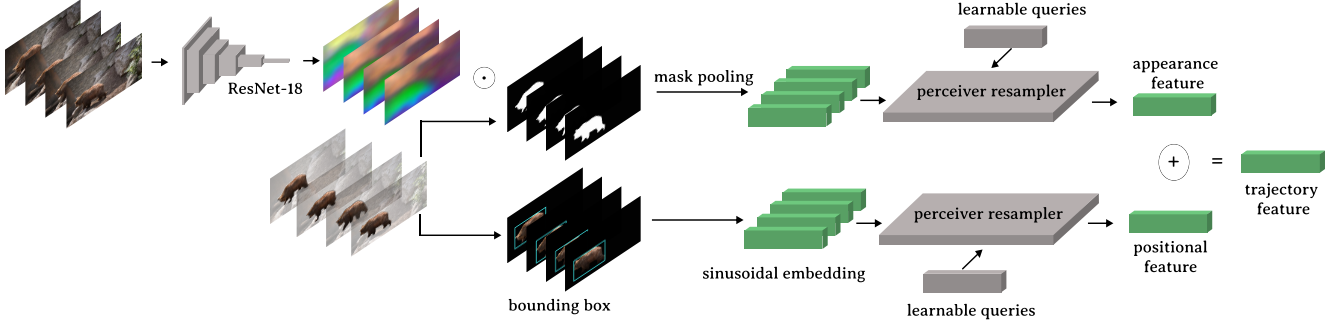


Figure 4. **Architecture of trajectory encoder.** we employ a two-branch design that encodes a trajectory’s appearance and temporal position separately. At each frame, we represent the appearance of a segment by mask pooling its feature, and represent its position by bounding box coordinates. Both features are then aggregated across frames via perceiver resampler and added together to form the trajectory feature.

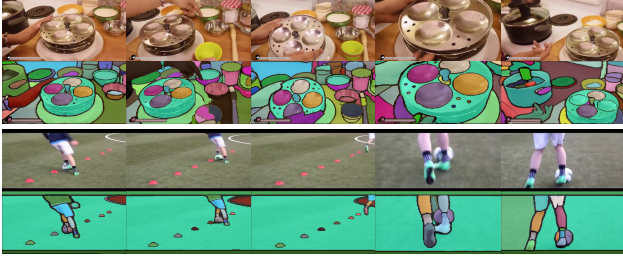


Figure 5. **Visualizations of generated trajectories.**

to obtain corresponding hierarchical feature maps $\{F_t\}_{t=1}^T$ for each frame. Then, for each trajectory, we extract its appearance feature via masked feature pooling. Specifically, for trajectory i at frame t , we compute:

$$f_t^i = \frac{\sum_{x,y} M_t^i(x,y) \cdot F_t(x,y)}{\sum_{x,y} M_t^i(x,y) + \epsilon} \quad (1)$$

where x,y denotes the spatial position, M_t^i is the trajectory’s segmentation mask, F_t is the feature map, and ϵ is a small constant. This operation pools the feature inside the region-of-interest for each trajectory. The resulting f_t^i represents the trajectory i ’s feature at frame t . Since a trajectory can span a varying number of frames, we need a mechanism to summarize a dynamic sequence of the per-frame features into a fixed-size embedding. We choose to use one layer of perceiver resampler module [1], which is a lightweight cross-attention layer that learns a predefined number of latent input queries to attend to the sequence of per-frame features. As we set the number of latent queries to be one, the perceiver resampler outputs a single embedding that serves as the appearance representation of the trajectory. We use rotary embedding [55] as the positional embedding of perceiver resampler module for better test-time frame number generalization.

Trajectory temporal position encoding. To represent the temporal position information of each trajectory, we extract bounding box coordinates $c_t^i = (x_1^i, y_1^i, x_2^i, y_2^i)$ at

each frame of the trajectory i . These coordinates are then mapped to high-dimensional vectors using sinusoidal embedding [41]. Since the bounding box sequence for a trajectory is also of variable length, we again employ the perceiver resampler module to summarize the sequence into a single temporal position embedding.

Finally, we construct the trajectory embedding by summing the appearance embedding and the temporal position embedding, which serves as a single token of the input to the transformer. The trajectory encoder has 20M parameters, much smaller than the transformer encoder (e.g., 304M for ViT-Large), yet can significantly reduce the number of tokens for efficient video processing, without dropping information in raw pixels.

Model Training. Our final video encoder *TrajViT* consists of this trajectory encoder followed by a standard transformer module. We train it with the CLIP objective [46]. Given a dataset of video-caption pairs, CLIP objective learn video and text representations by jointly training a video encoder and a text encoder with contrastive loss.

3.3. Seamless Integration with Image Data

Incorporating image data is a common practice when training video encoders, as the size of publicly available image data is several orders of magnitude larger than that of video data. *TrajViT* can integrate image data naturally without architectural modifications. Given an image, we apply the same segmentation process as in videos, and then treat each segmented region as a trajectory of length one. This enables seamless integration of image data into video pretraining. In contrast, models that use space-time patch tokenization cannot directly process image data because of their reliance on 3D convolutions or MLP layers that map space-time patches to fixed-size tokens. These modules require channel dimensions that match the spatial-temporal patch size, preventing direct image processing. As a result, space-time patch based approaches typically pretrain ViT2D on images, transfer the weights to ViT3D, and then fine-tune on video data, while

Model	ActivityNet		VATEX		MSR-VTT		Charades	
	txt2vid	vid2txt	txt2vid	vid2txt	txt2vid	vid2txt	txt2vid	vid2txt
ViT3D	35.3	34.5	<u>35.0</u>	<u>59.1</u>	<u>30.9</u>	56.5	12.9	12.6
TokenLearner	<u>36.9</u>	<u>36.8</u>	34.1	58.5	30.3	<u>58.7</u>	11.7	12.8
ViViT	33.4	32.9	34.0	57.9	29.5	54.6	12.0	12.3
AutoMerge	34.0	34.2	34.2	58.1	29.1	55.9	10.3	11.4
RLT	33.6	33.3	34.1	58.4	30.1	56.1	<u>13.4</u>	<u>12.8</u>
ToMe	31.4	31.4	34.0	56.6	28.6	55.31	10.2	10.5
TrajViT (ours)	38.6	38.4	36.2	61.0	31.7	61.0	14.9	14.8

Table 1. **Zero-shot video-text retrieval performance.** We report R@5 scores in four commonly used video retrieval datasets. Txt2vid stands for text-to-video while vid2txt stands for video-to-text. Our model consistently surpass all baselines by a large margin.

Model	AVAv2	ActivityNet		YouCook	
	mAP	txt2vid	vid2txt	txt2vid	vid2txt
ViT3D	<u>10.6</u>	39.3	42.3	46.8	50.0
TokenLearner	9.1	39.1	43.0	46.0	49.8
ViViT	9.9	38.9	42.3	45.7	48.8
AutoMerge	-	38.9	41.8	45.7	47.8
RLT	8.5	<u>39.3</u>	42.1	46.2	49.4
ToMe	8.3	38.4	42.0	45.4	48.2
TrajViT (ours)	13.7	39.6	<u>42.5</u>	47.2	50.0

Table 3. **Fine-grained video tasks.** AVAv2 is for spatial-temporal action detection task. ActivityNet and Youcook are for temporal clip retrieval task.

ours allows joint training on images and videos in one stage.

4. Experiments

We evaluate TrajViT on a diverse set of video understanding tasks. Our experiments cover three key areas: (1) general video understanding tasks that can be assessed directly using our trained CLIP model (Sec. 4.1); (2) model scaling behavior when the number of frames during inference or pretraining dataset size increases, as well as when image data is added to the pretraining corpus (Sec. 4.2); and (3) video-language QA tasks that can be evaluated by connecting a video encoder to an LLM (Sec. 4.3). We also include an ablation study in Sec. 4.4.

Training recipe. Models in the main experiments use the transformer architecture of ViT-Large [13] without pre-trained weights. During training, we uniformly sample a 16-frame clip from each video. All models are trained on a randomly sampled subset of the Panda-70M video captioning dataset [8]. We partition the dataset into three scales: 2M, 4M, and 8M video samples. TrajViT and ViT3D are trained on all three scales to analyze scaling performance, while all other baselines are trained on the 4M subset due to computational constraints. In one of our experiments that adds image data into pretraining, we use 50M randomly sampled image-text pairs from DataComp-1B [17] as the image dataset.

Baselines. We compare TrajViT with following baselines in

Model	K400	SSV2	UFC-101
ViT3D	<u>53.4</u>	46.1	<u>83.8</u>
TokenLearner	53.1	42.7	83.5
ViViT	51.0	43.0	<u>83.8</u>
AutoMerge	49.3	41.2	83.3
RLT	53.1	44.5	83.5
ToMe	50.3	41.7	82.9
TrajViT (ours)	55.6	<u>45.8</u>	84.5

Table 2. **Action classification performance.** Scores are reported in terms of top-1 accuracy. Our model is the only token merging method that is comparable with ViT3D’s performance.

a strict apple-to-apple manner, ensuring they share the same training dataset and recipe.

- **Space-time ViT (ViT3D):** A widely used baseline that tokenizes videos using fixed space-time patches and processes them with a standard transformer encoder [2].
- **AutoMerge:** A variant of our TrajViT which uses a learnable token merging mechanism on top of space-time patches to replace trajectory tokens. This serves as a control to study the impact of trajectory tokens (architecture detail in supplementary). We adjust its produced token count to match its FLOPS with that of TrajViT at 16-frame videos in the training set for a fair comparison.
- **Video token merging methods:** We compare with state-of-the-art token merging encoders such as ToMe [3], RLE [11], and TokenLearner [48], which reduce video token counts by dropping similar patches or intermediate patch features. We follow the default token reduction hyperparameters from the original papers for all methods.
- **Methods that modify transformer architectures:** We additionally include a widely-used video architecture ViViT [2], which improves video processing efficiency by modifying transformer design.

4.1. General Video Understanding Tasks

We first compare TrajViT against all baselines on a wide spectrum of general video understanding tasks that can be assessed by CLIP training, including action classification, video-text retrieval, and fine-grained spatial-temporal understanding. All models are trained on the 4M subset. We freeze the video encoders for all downstream evaluations. Unless otherwise specified, we uniformly sample 16 frames from videos as model input.

Video-text retrieval. We evaluate TrajViT on multiple video-text retrieval benchmarks, including ActivityNet-caption [25], Charades [51], MSR-VTT [64], and VATEX retrieval [61]. The evaluation is conducted in a zero-shot manner using our pretrained video and text encoder. As shown in Tab. 1, **TrajViT achieves a significant improvement over all baselines.** We attribute this to the nature of video-text retrieval tasks, where textual descriptions primarily focus on objects and their interactions. By leveraging

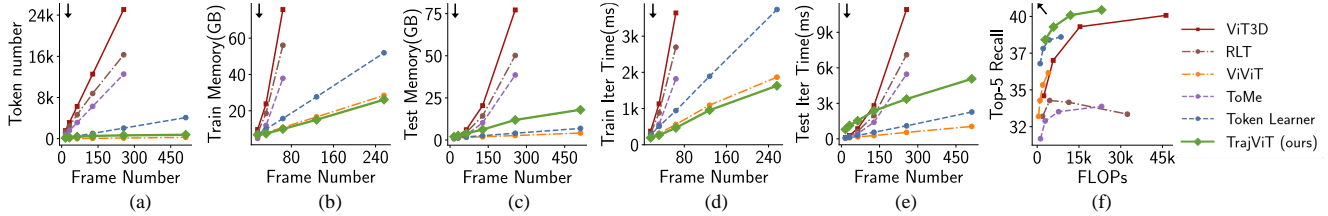


Figure 6. **Comparison of inference frame number scaling in ActivityNet video-to-text retrieval task.** Scaling with our tokenization paradigm obtains a better trade-off than baselines in terms of efficiency and accuracy.

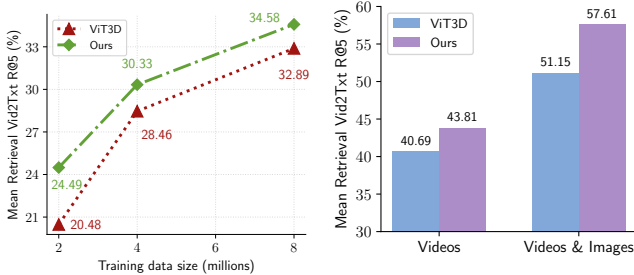


Figure 7. **Scaling video training data.** TrajViT maintains the lead over ViT3D across different scales of training data.

Figure 8. **Incorporating image data.** TrajViT benefits more from adding image data into pretraining as it requires no architectural modifications.

semantic tokens derived from object trajectories, TrajViT is better at identifying and matching objects, actions, and their relationships with the textual queries.

Action classification. We evaluate on three standard action recognition benchmarks: Something-Something V2 (SSV2) [18], Kinetics-400 (K400) [24], and UFC-101 [53]. Following prior works [62, 68, 72], we employ a multi-head attention probing (MAP) head to probe the output representations from video encoders. We also follow standard practice to aggregate predictions from 4 temporal views per video [2, 62, 68]. The results are presented in Tab. 2. **TrajViT outperforms all baselines on K400 and UCF-101.** On SSV2, our method significantly surpasses token merging approaches but slightly underperforms ViT3D. We observe that it might be because TrajViT generates very few tokens in SSV2 due to the relatively simple egocentric scene, which forces the model to over-compress complex motion in a single token.

Fine-grained spatial-temporal understanding. To assess TrajViT’s capability in recognizing fine-grained details in a video, we evaluate on spatial-temporal detection task at AVAv2 benchmark [19], as well as temporal clip retrieval task of ActivityNet [25] and YouCook [12] benchmarks. For spatial-temporal detection, we extract features from the region-of-interest and apply a MAP head to probe the action class (details in the supplementary) for each video encoder. For temporal clip retrieval, we follow [72] to repurpose

ActivityNet and YouCook for clip-to-text retrieval by segmenting each video into multiple clips based on the annotated timestamps. The retrieval task is then performed by selecting the correct description for a given video clip from the set of sequential descriptions within the same video. As shown in Tab. 3, **TrajViT outperforms all baselines by a large margin in spatial-temporal detection tasks.** We attribute this to the fact that our trajectory tokens maintain object consistency over time, leading to more precise spatial and temporal grounding. In temporal clip retrieval tasks, the performance gap between models is relatively small, possibly due to the presence of hard negatives that make the tasks challenging. However, TrajViT still ranks highest in most metrics, demonstrating its ability to effectively differentiate video segments.

4.2. Scaling Performance

We evaluate the scaling behavior of TrajViT along three axes: number of input frames, pretraining data size, and joint training with images.

Scaling the number of input frames. We examine how different models perform as the number of input frames T increases. We use the ActivityNet dense captioning retrieval task as our benchmark. This task requires retrieving long video clips ranging from 1 to 2 minutes, where incorporating more than 16 frames can help the model better align with the provided complex and densely annotated captions. We analyze both model performance and computational efficiency under varying temporal input lengths. For TrajViT, we note that generating trajectories is a one-time cost for a video: we precompute and store trajectories used for every training epoch. At inference, we consider both the trajectory generation and the model forward pass as part of TrajViT’s resource consumption.

We show results in Fig. 6. Compared to ViT3D, TrajViT scales effectively to a significantly larger number of frames while maintaining low resource consumption. We observe that TrajViT can generalize to more input frames with a smaller number of tokens (Fig. 6a), lower training GPU memory (Fig. 6b), and faster training iteration time (Fig. 6d). When taking trajectory generation overhead into account at inference, TrajViT runs faster only for videos

Model	NextQA		TempCompass				VideoMME	ActivityNetQA		MovieChat		MLVU
	OE	MC	MC	Yes/No	Cap.Match	Cap.	Acc.	Acc.	Score	Acc.	Score	Acc.
ViT3D	49.2	29.5	39.1	50.1	58.4	30.4	28.9	30.7	2.6	34.7	3.1	19.2
TrajViT	65.1	37.0	40.0	50.6	59.9	31.1	32.0	38.0	2.7	36.7	3.1	32.2

Table 4. **Comparison of ViT3D and TrajViT on VideoLLM QA tasks.** We report results on NextQA (WUPS score in open-ended subsets, accuracy in multi-choice subsets), TempCompass (accuracy for four subsets of multi-choice, yes/no, caption matching, and captioning), VideoMME (accuracy), MovieChat (accuracy and GPT score), ActivityNetQA (accuracy and GPT score), and MLVU (accuracy). The VideoLLM that uses our video encoder consistently outperforms the one with ViT3D across all video QA benchmarks.

with more than 64 frames (Fig. 6e), yet it consumes less GPU memory regardless of the number of frames (Fig. 6c). Most importantly, Fig. 6f demonstrates that **under the same computational cost, our approach consistently achieves better performance compared to all baselines.** These results highlight the potential of our design in building an efficient and strong long-term video understanding model. Note that the inference runtime and FLOPs of TrajViT are bottlenecked by the tracking pipeline, which is a potential direction to improve in our future work.

Scaling pretraining video data size. To examine how TrajViT scales with data, we train and compare TrajViT and ViT3D on 2M, 4M, and 8M video subsets of Panda70M. In Table 7, we report the average video-to-text retrieval performance across all four retrieval benchmarks from Sec. 4.1. **TrajViT consistently outperforms ViT3D across all three scales,** demonstrating equally strong scaling behavior. Interestingly, the performance gain at 2M is slightly larger than at 4M and 8M, possibly because the inductive biases introduced by our tokenization scheme provide greater benefits in lower-data regimes.

Incorporating image data. Most video encoders are initialized from image-pretrained models [2, 11, 27, 62, 72]. We investigate whether TrajViT can also benefit from image data. Unlike ViT3D, which requires separate image pretraining before video adaptation, TrajViT can be jointly trained on image and video data as discussed in Sec. 3.3. We conduct an experiment using the largest 8M video subset alongside the DataComp-50M image dataset [17]. We plot the average retrieval performance in Figure 8. Compared to ViT3D, **TrajViT achieves a larger performance boost when incorporating image data,** highlighting its ability to leverage image and video data more efficiently.

4.3. VideoLLM for QA tasks

We evaluate various VideoQA tasks by connecting TrajViT to the Llama-3 language model [36]. To focus on the impact of video encoders, we adopt the simple setup in [40]: A linear layer is used to connect the trained video encoder and LLM. We train two VideoLLM variants with ViT3D and TrajViT as video encoder (the variants that pretrained on 8M video data and 50M image data), and fine-tune the linear connector using the instruction tuning dataset from

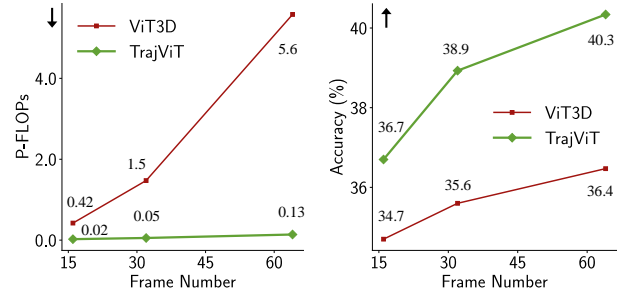


Figure 9. **Accuracy and inference FLOPs at MovieChat long video benchmarks with input frame scaling.** The VideoLLM with TrajViT as video encoder scales significantly better than the one with ViT3D in both accuracy and efficiency.

LlaVA-video [71]. We train both VideoLLMs for 3 epochs with a batch size of 32 and evaluate the models on various QA benchmarks, including VideoMME [16], NextQA [63], ActivityNetQA [67], MLVU [73], TempCompass [37], and MovieChat [52]. We follow the setup and evaluation metrics in the LMMs-Eval repository [28] for all benchmarks. The results are shown in Tab. 4. **TrajViT-LLM outperforms ViT3D-LLM across all QA benchmarks,** possibly because the modern VideoQA tasks often require reasoning about fine-grained objects and events in video, in which our trajectory-based tokenization helps. **TrajViT-LLM trains 4.2x faster and has 18x fewer inference FLOPs in average than ViT3D-LLM** because of the significantly fewer vision tokens proposed by our video encoder. Additionally, we specifically test how the trained VideoLLM performs in long videos by varying its input number of frames in MovieChat long video benchmark. We find that our model scales significantly better than ViT3D in both inference FLOPs and accuracy (Fig. 9), demonstrating its strong potential in building long-term video models.

4.4. Ablation Study

We conduct extensive ablations on the impact of segmentation and tracking, trajectory generation pipeline, and the trajectory encoder architecture. Due to computational constraints, all models in this study are trained on a randomly sampled 880k subset of Panda-70M, and we use ViT-Base

as the transformer backbone.

4.4.1. Impact of Segmentation and Tracking

When generating trajectories, our tokenization paradigm relies on segmentation and tracking models, both of which introduce unique inductive biases in generated tokens: segmentation reduces spatial redundancy and adds semantic information, while tracking reduces temporal redundancy. To understand their contributions, we analyze the individual impact of segmentation and tracking on model performance: the segmentation-only baseline segments each frame individually without considering temporal redundancy, while the tracking-only baseline performs tracking on 16x16 patches without segmentation. We use the patch tracking model in [21]. Both baselines use the same tokenizer architecture as TrajViT. As shown in Tab. 5, Both baselines underperform TrajViT. The segmentation-only model improves ViT3D on retrieval tasks but underperforms in both classification tasks, perhaps because spatially semantic tokens help the model better capture objects but fail to recognize actions due to the lack of temporal connections. Additionally, we find that patch-based tracking is not robust, as tracking in patches is less semantically meaningful than tracking object segments. This results in the patch-tracking model underperforming TrajViT.

4.4.2. Ablation of Trajectory Generation Pipeline

We ablate different design choices of the trajectory generation pipeline and show performance in Tab. 6.

Segmentation model. The model that uses segments from DirectSAM consistently outperforms the one with segments from SAM, likely due to DirectSAM’s ability to produce more detailed segmentation masks.

Trajectory resolution. Both DirectSAM and SAM2 are originally trained at a resolution of 1024. While using their original resolution provides more precise boundary in the generated masks, we observe minimal impact on downstream performance. Given the 4× reduction in compute, we adopt 512×512 resolution as our default setting.

Frame partitioning strategy. We find that using frame stride only underperforms in retrieval-related tasks, possibly because some objects in the mid-video fail to be detected at their first appearance. Using key frame only degrades performance in the SSV2 classification task. We suspect that this is because object changes rarely occur in SSV2, leading to very few detected key frames. As a result, each token is overloaded to represent lengthy trajectories.

4.4.3. Ablation of Trajectory Encoder Architecture

The ablations for different components of trajectory encoder architecture are shown in Tab. 6.

Feature extractor. Extracting features from ResNet-18 significantly outperform hierarchical transformer such as

Variation	SSV2	K400	Retrieval
<i>vit3d</i>	17.2	21.8	12.0
Segmentation-only	16.4	19.9	17.0
Tracking-only	19.3	18.1	15.4
TrajViT	22.7	25.9	17.8

Table 5. **Individual impact of segmentation and tracking.** We can see that removing segmentation (tracking-only) or tracking (segmentation-only) significantly hurts model performance.

	Objectives	Variation	SSV2	K400	Retrieval
		TrajViT	22.7	25.9	17.8
traj-gen	Resolution	1024→512	22.5 (↓ 0.2)	26.3 (↑ 0.4)	18.0 (↑ 0.2)
	Seg. Type	D-SAM→SAM	22.1 (↓ 0.6)	23.5 (↓ 2.4)	16.7 (↓ 1.1)
	Clip Par.	Key frame only Frame cut only	20.6 (↓ 2.1) 22.7 (0)	25.7 (↓ 0.2) 25.3 (↓ 0.6)	17.6 (↓ 0.2) 17.3 (↓ 0.5)
traj-encoder	Hiera. Feat.	Yes→No	22.4 (↓ 0.3)	25.1 (↓ 0.8)	17.5 (↓ 0.3)
	Pos. Branch	Yes→No	20.6 (↓ 2.1)	25.3 (↓ 0.6)	17.4 (↓ 0.4)
	ConvNet	ResNet→Hiera	18.3 (↓ 4.4)	21 (↓ 4.9)	16.0 (↓ 1.8)
	Feature Aggr.	Percei.→Mean	19.2 (↓ 3.5)	23.4 (↓ 2.5)	16.5 (↓ 1.3)
	Query Token	1→2 1→4	22.7 (0) 22.8 (↑ 0.1)	26.0 (↑ 0.1) 26.2 (↑ 0.3)	17.8 (0) 17.9 (↑ 0.1)

Table 6. **Ablation study of both trajectory generation pipeline and trajectory encoder architecture.**

Hiera-small, perhaps because convolutional filters provide better spatial features, especially for small modules.

Necessity of hierarchical features. Incorporating hierarchical features improves performance, likely because they help compensate for information loss during mask pooling operations when extracting region-specific features.

Necessity of the position branch. Although the appearance token may already encode some positional information from ResNet features, we find that an explicit position branch remains essential for strong performance.

Feature aggregation across frames. For aggregating per-frame features, we find that using perceiver resampler significantly outperforms simple mean-pooling, highlighting the importance of modeling temporal variation.

Number of query tokens per trajectory. Increasing the number of query tokens per trajectory provides only marginal performance improvements. This suggests that trajectory information is already heavily compressed before reaching the perceiver resampler. Addressing this potential bottleneck is left to future work.

5. Conclusion

We propose grounded video tokenization where tokens are built on panoptic sub-object trajectories and introduce TrajViT, a video encoder based on this new tokenization paradigm. In extensive video understanding experiments, TrajViT outperforms standard video tokenization in both accuracy and efficiency, while other token-efficient video encoders improve efficiency at the expense of accuracy.

References

- [1] Jean-Baptiste Alayrac, Jeff Donahue, Pauline Luc, Antoine Miech, Iain Barr, Yana Hasson, Karel Lenc, Arthur Mensch, Katherine Millican, Malcolm Reynolds, et al. Flamingo: a visual language model for few-shot learning. *Advances in neural information processing systems*, 35:23716–23736, 2022. 3, 4
- [2] Anurag Arnab, Mostafa Dehghani, Georg Heigold, Chen Sun, Mario Lučić, and Cordelia Schmid. Vivit: A video vision transformer. In *Proceedings of the IEEE/CVF international conference on computer vision*, pages 6836–6846, 2021. 1, 2, 5, 6, 7
- [3] Daniel Bolya, Cheng-Yang Fu, Xiaoliang Dai, Peizhao Zhang, Christoph Feichtenhofer, and Judy Hoffman. Token merging: Your vit but faster. *arXiv preprint arXiv:2210.09461*, 2022. 1, 2, 5
- [4] Shyamal Buch, Cristóbal Eyzaguirre, Adrien Gaidon, Jiajun Wu, Li Fei-Fei, and Juan Carlos Niebles. Re-visiting the” video” in video-language understanding. In *Proceedings of the IEEE/CVF conference on computer vision and pattern recognition*, pages 2917–2927, 2022. 2
- [5] Qingqing Cao, Bhargavi Paranjape, and Hannaneh Hajishirzi. PuMer: Pruning and merging tokens for efficient vision language models. In *Proceedings of the 61st Annual Meeting of the Association for Computational Linguistics (Volume 1: Long Papers)*, pages 12890–12903, Toronto, Canada, 2023. Association for Computational Linguistics. 2
- [6] Delong Chen, Samuel Cahyawijaya, Jianfeng Liu, Baoyuan Wang, and Pascale Fung. Subobject-level image tokenization. *arXiv preprint arXiv:2402.14327*, 2024. 2, 3
- [7] Liang Chen, Haozhe Zhao, Tianyu Liu, Shuai Bai, Junyang Lin, Chang Zhou, and Baobao Chang. An image is worth 1/2 tokens after layer 2: Plug-and-play inference acceleration for large vision-language models, 2024. 2
- [8] Tsai-Shien Chen, Aliaksandr Siarohin, Willi Menapace, Ekaterina Deyneka, Hsiang-wei Chao, Byung Eun Jeon, Yuwei Fang, Hsin-Ying Lee, Jian Ren, Ming-Hsuan Yang, et al. Panda-70m: Captioning 70m videos with multiple cross-modality teachers. In *Proceedings of the IEEE/CVF Conference on Computer Vision and Pattern Recognition*, pages 13320–13331, 2024. 2, 5
- [9] Ho Kei Cheng, Seoung Wug Oh, Brian Price, Joon-Young Lee, and Alexander Schwing. Putting the object back into video object segmentation. In *Proceedings of the IEEE/CVF Conference on Computer Vision and Pattern Recognition*, pages 3151–3161, 2024. 3
- [10] Joonmyung Choi, Sanghyeok Lee, Jaewon Chu, Minhyuk Choi, and Hyunwoo J. Kim. vid-tldr: Training free token merging for light-weight video transformer, 2024. 2
- [11] Rohan Choudhury, Guanglei Zhu, Sihan Liu, Koichiro Niinuma, Kris Kitani, and László Jeni. Don’t look twice: Faster video transformers with run-length tokenization. *Advances in Neural Information Processing Systems*, 37:28127–28149, 2025. 1, 2, 5, 7
- [12] Pradipto Das, Chenliang Xu, Richard F Doell, and Jason J Corso. A thousand frames in just a few words: Lingual description of videos through latent topics and sparse object stitching. In *Proceedings of the IEEE conference on computer vision and pattern recognition*, pages 2634–2641, 2013. 6
- [13] Alexey Dosovitskiy, Lucas Beyer, Alexander Kolesnikov, Dirk Weissenborn, Xiaohua Zhai, Thomas Unterthiner, Mostafa Dehghani, Matthias Minderer, Georg Heigold, Sylvain Gelly, et al. An image is worth 16x16 words: Transformers for image recognition at scale. *arXiv preprint arXiv:2010.11929*, 2020. 5
- [14] Mohsen Fayyaz, Soroush Abbasi Koohpayegani, Farnoush Rezaei Jafari, Sunando Sengupta, Hamid Reza Vaezi Joze, Eric Sommerlade, Hamed Pirsiavash, and Juergen Gall. Adaptive token sampling for efficient vision transformers, 2022. 2
- [15] Christoph Feichtenhofer, Haoqi Fan, Yanghao Li, and Kaiming He. Masked autoencoders as spatiotemporal learners, 2022. 2
- [16] Chaoyou Fu, Yuhang Dai, Yongdong Luo, Lei Li, Shuhuai Ren, Renrui Zhang, Zihan Wang, Chenyu Zhou, Yunhang Shen, Mengdan Zhang, et al. Videomme: The first-ever comprehensive evaluation benchmark of multi-modal llms in video analysis. *arXiv preprint arXiv:2405.21075*, 2024. 7
- [17] Samir Yitzhak Gadre, Gabriel Ilharco, Alex Fang, Jonathan Hayase, Georgios Smyrnis, Thao Nguyen, Ryan Marten, Mitchell Wortsman, Dhruva Ghosh, Jieyu Zhang, et al. Datacomp: In search of the next generation of multimodal datasets. *Advances in Neural Information Processing Systems*, 36:27092–27112, 2023. 5, 7
- [18] Raghav Goyal, Samira Ebrahimi Kahou, Vincent Michalski, Joanna Materzynska, Susanne Westphal, Heuna Kim, Valentin Haenel, Ingo Fruend, Peter Yianilos, Moritz Mueller-Freitag, et al. The” something something” video database for learning and evaluating visual common sense. In *Proceedings of the IEEE international conference on computer vision*, pages 5842–5850, 2017. 6
- [19] Chunhui Gu, Chen Sun, David A Ross, Carl Vondrick, Caroline Pantofaru, Yeqing Li, Sudheendra Vijayanarasimhan, George Toderici, Susanna Ricco, Rahul Sukthankar, et al. Ava: A video dataset of spatio-

- temporally localized atomic visual actions. In *Proceedings of the IEEE conference on computer vision and pattern recognition*, pages 6047–6056, 2018. 6
- [20] Kaiming He, Xiangyu Zhang, Shaoqing Ren, and Jian Sun. Deep residual learning for image recognition. In *Proceedings of the IEEE conference on computer vision and pattern recognition*, pages 770–778, 2016. 3
- [21] Allan Jabri, Andrew Owens, and Alexei Efros. Space-time correspondence as a contrastive random walk. *Advances in neural information processing systems*, 33:19545–19560, 2020. 8
- [22] Andrew Jaegle, Felix Gimeno, Andy Brock, Oriol Vinyals, Andrew Zisserman, and Joao Carreira. Perceiver: General perception with iterative attention. In *International conference on machine learning*, pages 4651–4664. PMLR, 2021. 3
- [23] Yang Jin, Zhicheng Sun, Kun Xu, Kun Xu, Liwei Chen, Hao Jiang, Quzhe Huang, Chengru Song, Yuliang Liu, Di Zhang, Yang Song, Kun Gai, and Yadong Mu. Video-lavit: Unified video-language pre-training with decoupled visual-motional tokenization, 2024. 2
- [24] Will Kay, Joao Carreira, Karen Simonyan, Brian Zhang, Chloe Hillier, Sudheendra Vijayanarasimhan, Fabio Viola, Tim Green, Trevor Back, Paul Natsev, et al. The kinetics human action video dataset. *arXiv preprint arXiv:1705.06950*, 2017. 6
- [25] Ranjay Krishna, Kenji Hata, Frederic Ren, Li Fei-Fei, and Juan Carlos Niebles. Dense-captioning events in videos. In *Proceedings of the IEEE international conference on computer vision*, pages 706–715, 2017. 5, 6
- [26] Jie Lei, Linjie Li, Luwei Zhou, Zhe Gan, Tamara L Berg, Mohit Bansal, and Jingjing Liu. Less is more: Clipbert for video-and-language learning via sparse sampling. In *Proceedings of the IEEE/CVF conference on computer vision and pattern recognition*, pages 7331–7341, 2021. 2
- [27] Jie Lei, Tamara L Berg, and Mohit Bansal. Revealing single frame bias for video-and-language learning. *arXiv preprint arXiv:2206.03428*, 2022. 2, 7
- [28] Bo Li, Peiyuan Zhang, Kaichen Zhang, Fanyi Pu, Xinrun Du, Yuhao Dong, Haotian Liu, Yuanhan Zhang, Ge Zhang, Chunyuan Li, and Ziwei Liu. Lmms-eval: Accelerating the development of large multimodal models, 2024. 7
- [29] Junnan Li, Dongxu Li, Silvio Savarese, and Steven Hoi. Blip-2: Bootstrapping language-image pre-training with frozen image encoders and large language models, 2023. 3
- [30] KunChang Li, Yinan He, Yi Wang, Yizhuo Li, Wenhai Wang, Ping Luo, Yali Wang, Limin Wang, and Yu Qiao. Videochat: Chat-centric video understanding, 2024. 3
- [31] Kunchang Li, Xinhao Li, Yi Wang, Yinan He, Yali Wang, Limin Wang, and Yu Qiao. Videomamba: State space model for efficient video understanding, 2024. 2
- [32] Yi Li, Kyle Min, Subarna Tripathi, and Nuno Vasconcelos. Svtt: Temporal learning of sparse video-text transformers. In *Proceedings of the IEEE/CVF Conference on Computer Vision and Pattern Recognition*, pages 18919–18929, 2023. 2
- [33] Yanwei Li, Chengyao Wang, and Jiaya Jia. Llama-vid: An image is worth 2 tokens in large language models, 2023. 2, 3
- [34] Youwei Liang, Chongjian Ge, Zhan Tong, Yibing Song, Jue Wang, and Pengtao Xie. Not all patches are what you need: Expediting vision transformers via token reorganizations. *arXiv preprint arXiv:2202.07800*, 2022. 2
- [35] Kevin Lin, Linjie Li, Chung-Ching Lin, Faisal Ahmed, Zhe Gan, Zicheng Liu, Yumao Lu, and Lijuan Wang. Swinbert: End-to-end transformers with sparse attention for video captioning. In *Proceedings of the IEEE/CVF conference on computer vision and pattern recognition*, pages 17949–17958, 2022. 1
- [36] Ruyang Liu, Haoran Tang, Haibo Liu, Yixiao Ge, Ying Shan, Chen Li, and Jiankun Yang. Ppllava: Varied video sequence understanding with prompt guidance. *arXiv preprint arXiv:2411.02327*, 2024. 7
- [37] Yuanxin Liu, Shicheng Li, Yi Liu, Yuxiang Wang, Shuhuai Ren, Lei Li, Sishuo Chen, Xu Sun, and Lu Hou. Tempcompass: Do video llms really understand videos? *arXiv preprint arXiv:2403.00476*, 2024. 7
- [38] Ilya Loshchilov and Frank Hutter. Decoupled weight decay regularization. *arXiv preprint arXiv:1711.05101*, 2017. 1
- [39] Huaishao Luo, Lei Ji, Ming Zhong, Yang Chen, Wen Lei, Nan Duan, and Tianrui Li. Clip4clip: An empirical study of clip for end to end video clip retrieval, 2021. 2
- [40] Muhammad Maaz, Hanoona Rasheed, Salman Khan, and Fahad Shahbaz Khan. Video-chatgpt: Towards detailed video understanding via large vision and language models. *arXiv preprint arXiv:2306.05424*, 2023. 7
- [41] Ben Mildenhall, Pratul P Srinivasan, Matthew Tancik, Jonathan T Barron, Ravi Ramamoorthi, and Ren Ng. Nerf: Representing scenes as neural radiance fields for view synthesis. *Communications of the ACM*, 65(1): 99–106, 2021. 4
- [42] Arsha Nagrani, Shan Yang, Anurag Arnab, Aren Jansen, Cordelia Schmid, and Chen Sun. Attention bottlenecks for multimodal fusion. In *Advances*

- in *Neural Information Processing Systems*, pages 14200–14213. Curran Associates, Inc., 2021. 2
- [43] Daniel Neimark, Omri Bar, Maya Zohar, and Dotan Asselmann. Video transformer network. In *Proceedings of the IEEE/CVF international conference on computer vision*, pages 3163–3172, 2021. 1
- [44] Bowen Pan, Rameswar Panda, Yifan Jiang, Zhangyang Wang, Rogerio Feris, and Aude Oliva. Ia-red²: Interpretability-aware redundancy reduction for vision transformers, 2021. 2
- [45] Zenon W Pylyshyn and Ron W Storm. Tracking multiple independent targets: Evidence for a parallel tracking mechanism. *Spatial vision*, 3(3):179–197, 1988. 1
- [46] Alec Radford, Jong Wook Kim, Chris Hallacy, Aditya Ramesh, Gabriel Goh, Sandhini Agarwal, Girish Sastry, Amanda Askell, Pamela Mishkin, Jack Clark, et al. Learning transferable visual models from natural language supervision. In *International conference on machine learning*, pages 8748–8763. PMLR, 2021. 2, 4
- [47] Nikhila Ravi, Valentin Gabeur, Yuan-Ting Hu, Ronghang Hu, Chaitanya Ryali, Tengyu Ma, Haitham Khedr, Roman Rädle, Chloe Rolland, Laura Gustafson, et al. Sam 2: Segment anything in images and videos. *arXiv preprint arXiv:2408.00714*, 2024. 2, 3
- [48] Michael S Ryoo, AJ Piergiovanni, Anurag Arnab, Mostafa Dehghani, and Anelia Angelova. Token-learner: What can 8 learned tokens do for images and videos? *arXiv preprint arXiv:2106.11297*, 2021. 1, 2, 5
- [49] Xiaoqian Shen, Yunyang Xiong, Changsheng Zhao, Lemeng Wu, Jun Chen, Chenchen Zhu, Zechun Liu, Fanyi Xiao, Balakrishnan Varadarajan, Florian Bordes, Zhuang Liu, Hu Xu, Hyunwoo J. Kim, Bilge Soran, Raghuraman Krishnamoorthi, Mohamed Elhoseiny, and Vikas Chandra. Longvu: Spatiotemporal adaptive compression for long video-language understanding. *arXiv preprint arXiv:2410.17434*, 2024. 3
- [50] Yan Shu, Zheng Liu, Peitian Zhang, Minghao Qin, Junjie Zhou, Zhengyang Liang, Tiejun Huang, and Bo Zhao. Video-xl: Extra-long vision language model for hour-scale video understanding, 2024. 2
- [51] Gunnar A Sigurdsson, Gül Varol, Xiaolong Wang, Ali Farhadi, Ivan Laptev, and Abhinav Gupta. Hollywood in homes: Crowdsourcing data collection for activity understanding. In *Computer Vision—ECCV 2016: 14th European Conference, Amsterdam, The Netherlands, October 11–14, 2016, Proceedings, Part I 14*, pages 510–526. Springer, 2016. 5
- [52] Enxin Song, Wenhao Chai, Guanhong Wang, Yucheng Zhang, Haoyang Zhou, Feiyang Wu, Haozhe Chi, Xun Guo, Tian Ye, Yanting Zhang, et al. Moviechat: From dense token to sparse memory for long video understanding. In *Proceedings of the IEEE/CVF Conference on Computer Vision and Pattern Recognition*, pages 18221–18232, 2024. 2, 7
- [53] Khurram Soomro, Amir Roshan Zamir, and Mubarak Shah. Ucf101: A dataset of 101 human actions classes from videos in the wild. *arXiv preprint arXiv:1212.0402*, 2012. 6
- [54] Elizabeth S Spelke. Principles of object perception. *Cognitive science*, 14(1):29–56, 1990. 1
- [55] Jianlin Su, Murtadha Ahmed, Yu Lu, Shengfeng Pan, Wen Bo, and Yunfeng Liu. Roformer: Enhanced transformer with rotary position embedding. *Neuro-computing*, 568:127063, 2024. 4
- [56] Cisco Systems. Global device growth and traffic profiles. Technical report, Cisco, 2018. Accessed: 2024-11-29. 1
- [57] Zhan Tong, Yibing Song, Jue Wang, and Limin Wang. Videomae: Masked autoencoders are data-efficient learners for self-supervised video pre-training. *Advances in neural information processing systems*, 35: 10078–10093, 2022. 2
- [58] A Vaswani. Attention is all you need. *Advances in Neural Information Processing Systems*, 2017. 1
- [59] Johan Wagemans, James H Elder, Michael Kubovy, Stephen E Palmer, Mary A Peterson, Manish Singh, and Rüdiger Von der Heydt. A century of gestalt psychology in visual perception: I. perceptual grouping and figure-ground organization. *Psychological bulletin*, 138(6):1172, 2012. 1
- [60] Junke Wang, Xitong Yang, Hengduo Li, Liu Li, Zuxuan Wu, and Yu-Gang Jiang. Efficient video transformers with spatial-temporal token selection. In *ECCV*, 2022. 2
- [61] Xin Wang, Jiawei Wu, Junkun Chen, Lei Li, Yuanfang Wang, and William Yang Wang. Vatex: A large-scale, high-quality multilingual dataset for video-and-language research. In *Proceedings of the IEEE/CVF international conference on computer vision*, pages 4581–4591, 2019. 5
- [62] Yi Wang, Kunchang Li, Xinhao Li, Jiashuo Yu, Yinan He, Guo Chen, Baoqi Pei, Rongkun Zheng, Zun Wang, Yansong Shi, et al. Internvideo2: Scaling foundation models for multimodal video understanding. In *European Conference on Computer Vision*, pages 396–416. Springer, 2024. 6, 7
- [63] Junbin Xiao, Xindi Shang, Angela Yao, and Tat-Seng Chua. Next-qa: Next phase of question-answering to explaining temporal actions. In *Proceedings of the IEEE/CVF conference on computer vision and pattern recognition*, pages 9777–9786, 2021. 7

- [64] Jun Xu, Tao Mei, Ting Yao, and Yong Rui. Msr-vtt: A large video description dataset for bridging video and language. In *Proceedings of the IEEE conference on computer vision and pattern recognition*, pages 5288–5296, 2016. [5](#)
- [65] Jinyu Yang, Mingqi Gao, Zhe Li, Shang Gao, Fangjing Wang, and Feng Zheng. Track anything: Segment anything meets videos. *arXiv preprint arXiv:2304.11968*, 2023. [3](#)
- [66] Senqiao Yang, Yukang Chen, Zhuotao Tian, Chengyao Wang, Jingyao Li, Bei Yu, and Jiaya Jia. Visionzip: Longer is better but not necessary in vision language models, 2024. [2](#)
- [67] Zhou Yu, Dejing Xu, Jun Yu, Ting Yu, Zhou Zhao, Yueting Zhuang, and Dacheng Tao. Activitynet-qa: A dataset for understanding complex web videos via question answering. In *Proceedings of the AAAI Conference on Artificial Intelligence*, pages 9127–9134, 2019. [7](#)
- [68] Liangzhe Yuan, Nitesh Bharadwaj Gundavarapu, Long Zhao, Hao Zhou, Yin Cui, Lu Jiang, Xuan Yang, Menglin Jia, Tobias Weyand, Luke Friedman, et al. Videoglue: Video general understanding evaluation of foundation models. *arXiv preprint arXiv:2307.03166*, 2023. [6](#)
- [69] Boqiang Zhang, Kehan Li, Zesen Cheng, Zhiqiang Hu, Yuqian Yuan, Guanzheng Chen, Sicong Leng, Yuming Jiang, Hang Zhang, Xin Li, Peng Jin, Wenqi Zhang, Fan Wang, Lidong Bing, and Deli Zhao. Videollama 3: Frontier multimodal foundation models for image and video understanding, 2025. [2](#)
- [70] Shaolei Zhang, Qingkai Fang, Zhe Yang, and Yang Feng. Llava-mini: Efficient image and video large multimodal models with one vision token, 2025. [2](#)
- [71] Yuanhan Zhang, Jinming Wu, Wei Li, Bo Li, Zejun Ma, Ziwei Liu, and Chunyuan Li. Video instruction tuning with synthetic data. *arXiv preprint arXiv:2410.02713*, 2024. [7](#)
- [72] Long Zhao, Nitesh B Gundavarapu, Liangzhe Yuan, Hao Zhou, Shen Yan, Jennifer J Sun, Luke Friedman, Rui Qian, Tobias Weyand, Yue Zhao, et al. Video-prism: A foundational visual encoder for video understanding. *arXiv preprint arXiv:2402.13217*, 2024. [6](#), [7](#)
- [73] Junjie Zhou, Yan Shu, Bo Zhao, Boya Wu, Shitao Xiao, Xi Yang, Yongping Xiong, Bo Zhang, Tiejun Huang, and Zheng Liu. Mlvu: A comprehensive benchmark for multi-task long video understanding. *arXiv preprint arXiv:2406.04264*, 2024. [7](#)

One Trajectory, One Token: Grounded Video Tokenization via Panoptic Sub-object Trajectory

Supplementary Material

6. More Implementation Details

We provide the complete training details in Table 7. We optimize the models using AdamW optimizer [38] with a learning rate of 10^{-4} , a weight decay of 10^{-2} , and mixed precision training. We adopt a cosine annealing learning rate schedule. The contrastive view (batch size) for video training is set to 256, and all models are trained for 30 epochs. We train all models with 32 NVIDIA H100 GPUs. For data augmentation, we apply a combination of random ColorJitter, Grayscale, Gaussian blur, horizontal flip, and resized cropping during training. At testing, we use only a simple resizing operation to ensure consistency.

Hyperparameters for downstream MAP probing. For two downstream evaluations that require MAP probing, We use AdamW optimizer with weight decay 0.5, and set learning rate to be 0.0001. We also layer-normalize the video features before providing them to the classifier. We use a batch size of 128, and we train the classifier for 12 epochs.

Hyperparameter	Value
Trasformer size	vit-large
Resolution	224
Frame sampling	uniform 16 frames
Optimizer	AdamW
Base LR	$1e^{-4}$
Weight decay	0.02
Optimizer momentum	$\beta_1 = 0.9, \beta_2 = 0.999$
Batch size	video-256, image-4096
Training epochs	30
LR schedule	cosine decay
Warm up epochs	1
Warm up schedule	linear warm-up
Random crop scale	(0.2, 1.0)
Random crop ratio	(3/4, 4/3)
Horizontal flip probability	0.5
Color jitter probability	0.8
Gaussian blur probability	0.5
Grayscale probability	0.2

Table 7. hyperparameters used for pre-training.

7. More Architecture Details

To complement the main paper, we provide additional details on our model architecture and TokenMerge baseline’s

architecture.

Trajectory Encoder. We provide the complete architectural details of our trajectory tokenizer in table ???. As shown, the parameter size of our tokenizer is an order of magnitude smaller compared with main transformer.

TokenMerge Baseline. Although the size of our trajectory encoder is very small (20M) compared with the transformer encoder (304M), to ensure that our improvements do not simply come from adding parameters, we train a model that uses exactly the same modules as TrajViT but uses a learnable token merging mechanism that does not incorporate trajectory priors. The architecture of the TokenMerge baseline is illustrated in Figure 10. We design it such that the only difference from our trajectory tokenizer is whether it incorporates trajectory priors when compressing tokens. All other architectural modules remain identical to ensure a controlled comparison. The output token number is set to be 1024 to match the average FLOPs of our model at training set (including trajectory generation).

8. Key Frame Detection Algorithm

We illustrate the details of our key frame detection algorithm, which ensembles three sub-detectors to ensure robust scene boundary identification. A frame is classified as a key frame if it is proposed by at least two out of the three detectors. All detectors are implemented using the Content-Aware Detector from the PySceneDetect package.

HSV Colorspace Detector. This detector operates in the HSV color space. Each frame is converted from RGB to HSV, and the average difference across all channels is computed frame by frame. A scene change is triggered if the difference between adjacent frames exceeds threshold 27.

Luminance Histogram Detector. Each frame is converted from its original color space to YCbCr, and the Y channel (luminance) is extracted. The normalized histogram of the Y channel in the current frame is then compared to that of the previous frame using the correlation method (cv2.HISTCM_CORREL). A scene change is detected if the histogram correlation between consecutive frames falls below a set threshold 0.15.

RGB Detector. This detector computes an intensity value for each frame by averaging the R, G, and B values across all pixels, yielding a single floating-point number. A scene cut is triggered if the intensity difference between consecutive frames exceeds threshold 12.

Module	Detail	Output Shape	Parameter Size
Per-frame Feature Extractor	sum $\left\{ \begin{array}{l} \text{ResNet18 stage 1 + linear (64} \rightarrow \text{64) + resize (56} \times \text{56)} \\ \text{ResNet18 stage 2 + linear (128} \rightarrow \text{64) + resize (28} \rightarrow \text{56)} \\ \text{ResNet18 stage 3 + linear (256} \rightarrow \text{64) + resize (14} \rightarrow \text{56)} \\ \text{ResNet18 stage 4 + linear (512} \rightarrow \text{64) + resize (7} \rightarrow \text{56)} \end{array} \right\}$	$T \times 56 \times 56 \times 64$	11.6M
Mask Pooling	Mask pooling per trajectory (total N trajectories)	$N \times T \times 64$	0
Sinusoidal Encoder	bounding box coordinate (4) \rightarrow high-dimensional embeddings (64)	$N \times T \times 64$	0
Perceiver Resampler	Multi-head cross attention $\left\{ \begin{array}{l} \text{Query: 1; Layers: 1} \\ \text{Heads: 8; Dim: 64} \end{array} \right\} \times 2$	$N \times T \times 64$	8.4M
MLP	Linear (64 \rightarrow 1024) $\times 2$	$N \times 1024$	0.13M
Main Transformer	Transformer module of ViT-Large	$N \times 1024$	304M

Table 8. Detailed architecture of our model.

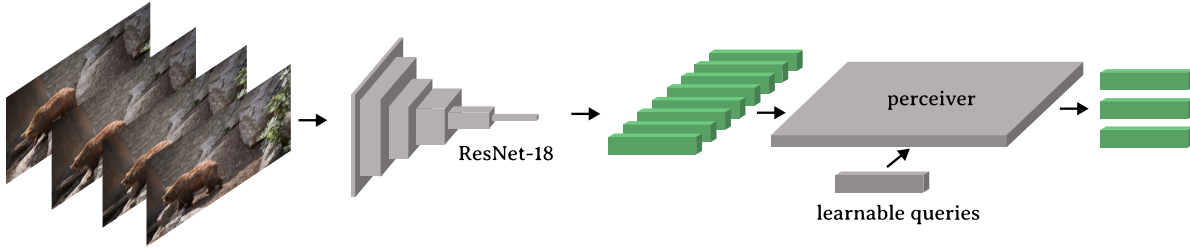


Figure 10. Architecture for TokenMerge baseline.

Model	K400	SSV2	UFC-101
ViT3D	<u>42.0</u>	12.3	<u>40.4</u>
TokenLearner	40.9	11.0	37.8
ViViT	39.9	11.5	34.8
AutoMerge	38.4	10.3	35.4
RLT	41.0	10.3	33.7
ToMe	38.2	9.9	37.1
TrajViT (ours)	42.4	<u>11.8</u>	42.1

Table 9. **Zero-shot action classification performance.** We report top-5 accuracy.

9. Detailed setup in AVAv2 Spatial Temporal Detection task

We follow the setup in [57] to evaluate our model on the AVAv2 spatial-temporal action detection task. In this task, given an object’s bounding box in a specific video frame, the model must predict the action associated with that object at that time instant. This requires extracting video features corresponding to the region of interest (ROI) and applying a probing head to classify the action based on the localized features. We use the same attentive probing head across all models, but the ROI pooling strategy differs depending on each model’s tokenization mechanism, which we illustrate below:

ViT3D. ViT3D produces a spatial-temporal feature map, al-

lowing us to use ROIAlign to extract features corresponding to the given bounding box. This setup is the same as [57]

Our Model. Since each output token in our model corresponds to an object trajectory, we leverage its segmentation mask at each timestep to determine its presence within the bounding box. We gather all tokens whose trajectories have at least 80% of their segmentation mask area inside the bounding box at the annotated frame.

ViViT. ViViT is a two-stage model, where the first stage outputs spatial features, and the second stage extracts temporal features. We handle this by pooling its spatial features using ROIAlign and selecting the corresponding temporal feature based on the annotated timestep. The final feature is obtained by concatenating the pooled spatial and temporal representations.

TokenLearner. We use the TokenFuser module proposed in its original paper to reproject pruned tokens back to their original spatial locations. This allows us to perform feature pooling in the same manner as ViT3D.

RLT & ToMe. Both RLT and ToMe dynamically merge space-time patch tokens that are identified as redundant. We reassemble the feature map by duplicating merged features back to their corresponding redundant patches, then ROI pool the reconstructed feature map in the same way as ViT3D.

TokenMerge. Since TokenMerge learns to merge tokens in a fully data-driven manner, it does not retain explicit spatial correspondences to the original input grid. As a result, we

Training Data	Model	ActivityNet		VATEX		MSR-VTT		Charades	
		txt2vid	vid2txt	txt2vid	vid2txt	txt2vid	vid2txt	txt2vid	vid2txt
panda-2m	ViT3D	26.33	27.33	24.74	44.80	23.75	48.30	7.11	7.29
	TrajViT (ours)	31.97	31.97	28.94	51.40	26.94	50.60	10.14	10.47
panda-4m	ViT3D	35.34	34.54	35.00	59.11	30.90	56.61	12.61	12.61
	TrajViT (ours)	38.62	38.41	36.19	61.02	31.71	60.52	14.81	14.81
panda-8m	ViT3D	38.82	37.46	40.59	64.46	34.71	60.83	17.45	16.00
	TrajViT (ours)	42.35	41.92	41.35	65.35	35.22	62.73	19.41	18.36

Table 10. **Full retrieval performance for pretraining video data scaling experiment.** We report results on four commonly used video retrieval datasets for both text-to-video (txt2vid) and video-to-text (vid2txt).

Training Data	Model	ActivityNet		VATEX		MSR-VTT		Charades	
		txt2vid	vid2txt	txt2vid	vid2txt	txt2vid	vid2txt	txt2vid	vid2txt
panda8m	ViT3D	37.82	34.54	39.59	59.11	33.71	56.51	15.35	12.61
	TrajViT (ours)	41.35	38.41	40.35	61.02	34.22	61.00	18.41	14.81
panda8m + datacomp50m	ViT3D	43.62	44.65	47.16	70.70	41.16	68.74	21.25	20.50
	TrajViT (ours)	53.57	53.36	50.38	75.10	47.38	79.96	24.80	22.01

Table 11. **Full retrieval performance for incorporating image data experiment.** We report R@5 scores on four commonly used video retrieval datasets. txt2vid is text-to-video retrieval and vid2txt is video-to-text retrieval.

Model	ImageNet		COCO	
	Top-5 Acc	img2txt R@5	txt2img R@5	
ViT	77.7	73.6	58.3	
TrajViT (ours)	74.9	71.1	55.5	

Table 12. **Performance for image-only experiments.** We report top-5 accuracy for ImageNet classification and Recall@5 for COCO retrieval (image-to-text & text-to-image).

are unable to pool features corresponding to the region of interest.

10. Full tables for scaling performance experiments

We provide the complete table for the scaling up experiments, which we only show the plots of average trend in the main table. Table 10 presents the performance variations of the model with the change of the scale of the training data. Table 11 presents the model’s performance with images adding to training data.

11. Zero-shot action classification

We report zero-shot action classification performance for all models here as a complement for attentive probing action classification that shown in the main paper. We note that for video model, attentive probing that only involves vision

encoder is a more accurate measure for action classification task, because the text template for action is hard to construct and likely to be out-of-distribution for text that model saw during training (e.g. put something on something). Nevertheless, as shown in table 9, our model still has competitive performance under zero-shot setting, outperforming most of baseline models.

12. Visualizations of generated trajectories

We show examples of generated trajectories in our training set at figure 11 and figure 12. Our pipeline allows us to generate high-quality panoptic trajectory with high efficiency. The generated segments are in detailed subobject level, allowing us to reason fine-grained interaction. The tracking is also very robust attributing to the powerful SAM2 model. We do observe occasional matching failure for the same objects between sub-clips (like frame 3→ 4 in example 3), causing the same object being split into multiple trajectories.

13. Image only experiments

Since we mention our model can naturally be adapted to image data, it will be interesting to see its performance in image-only training as well. We therefore train our model at datacomp50M image-captioning dataset, and compare it to regular ViT model that trains in the same dataset (table 12. We found our model underperforms ViT in down-

stream evaluation of ImageNet zero-shot classification and COCO zero-shot image-text retrieval. This means our bigger gain in incorporating image data experiment for our model is primarily because our model can train at image and video together, avoiding image-then-video pipeline and the information loss when transferring 2D model's weight to 3D model. How to improve our model design to let it become also competitive in image-only domain is left to future work.

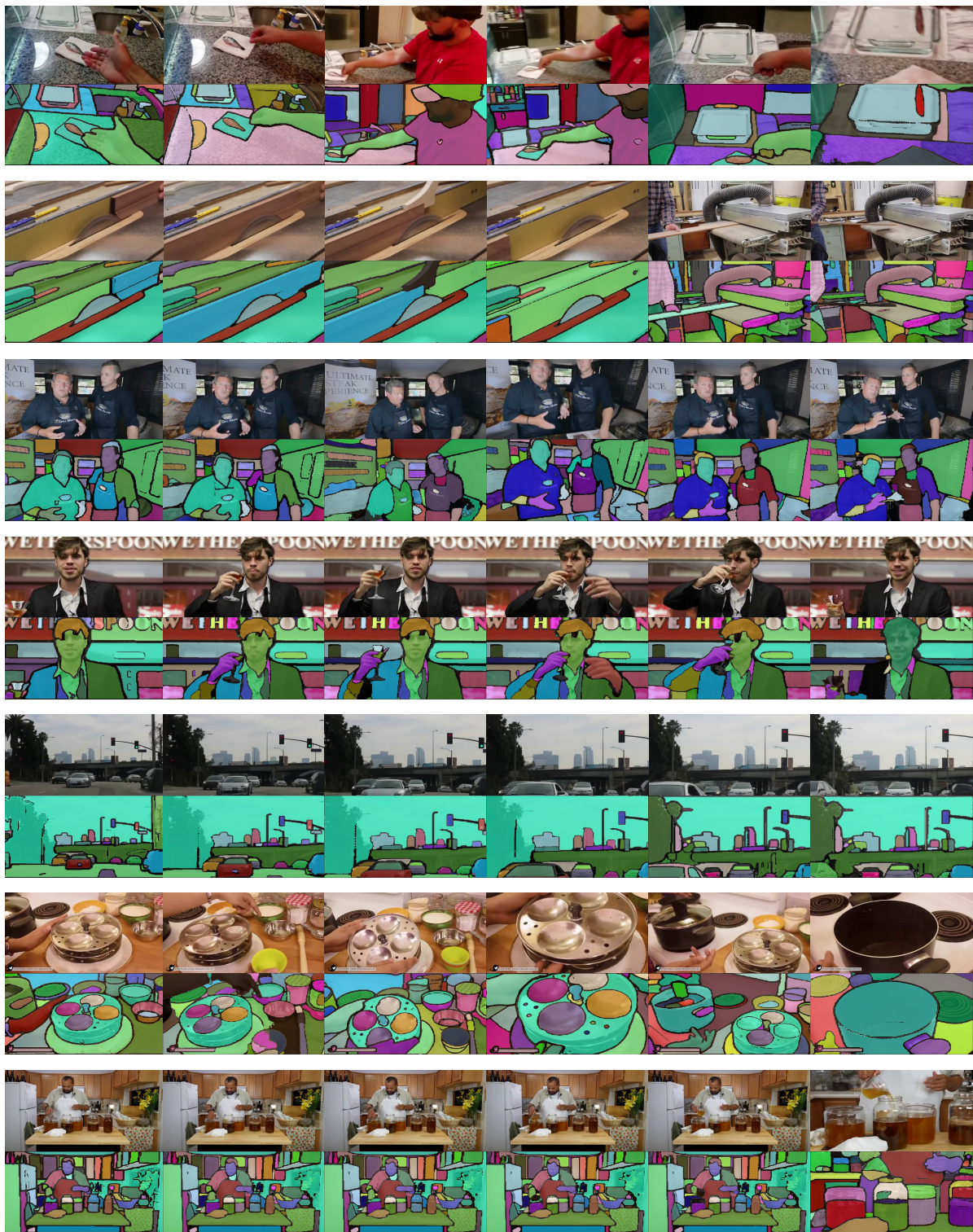


Figure 11. Visualizations of our generated trajectories (part 1).

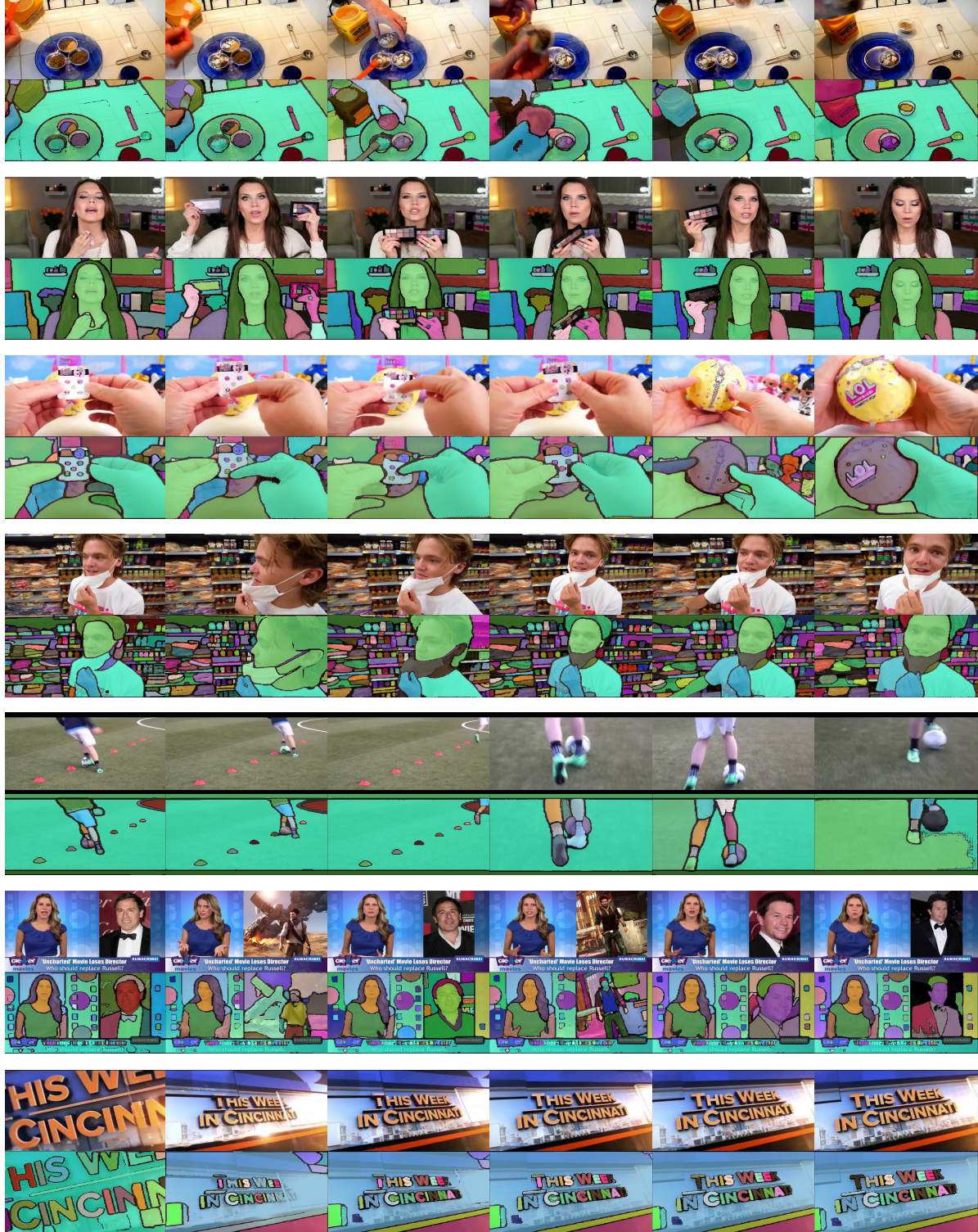


Figure 12. Visualizations of our generated trajectories (part 2).